Revista Brasileira de Geofísica; 1987, *Vol. 5, 29-41*

doi: 10.22564/rbgf.v5i1.1061

REDUCTION OF AMBIGUITY IN GEOELECTRIC MODELS USING MULTIPLE DATA SETS

A. RIGOTI

Instituto de Pesquisas Tecnológicas do Estado de São Paulo – S.A. – IPT
São Paulo, SP, Brazil

D.J. CROSSLEY

McGill University, Dept. of Geological Sciences, 3450
University Street, Montreal, P.Q., H3A 2A7, Canadá

DC-resistivity, time-domain IP and MT data are combined in an attempt to reduce the ambiguity inherent in each method. The known effectiveness of combined DC and MT resistivity is confirmed. Previous works are extended by adding apparent chargeability data.
The analysis of the IP data contribution renders difficult because of the inclusion of new parameters (chargeabilities) into the joint inversion, but even so it was possible to conclude that IP data also improve our confidence in model parameters, although to a lesser extent.
Even being aware of the benefits of combined MT – DC resistivity, a lower priced alternative, namely IP – resistivity was investigated in a field example. This combination presents advantages over resistivity alone due to the simple fact that a new related experiment is added to solve for the model parameters.
The main advantage of joint IP – rsistivity undoubtedly still resides in the possibillity of a single resistivity layer behaving as more than one IP layer, thus improving resolution.

Dados de resistividade DC, IP-domínio do tempo e MT são combinados para avaliar a redução da ambigüidade inerente a cada método. Confirma-se a já conhecida eficiência da combinação resistividade DC – MT e estendem-se estudos anteriores pela adição de dados de cargabilidade aparente.
A análise da contribuição dos dados IP é dificultada pela inclusão de novos parâmetros (cargabilidades) na inversão conjunta, mas mesmo assim fica claro que os dados de cargabilidade também melhoram a resolução do modelo geoelétrico, embora em menor grau.
Mesmo conhecendo as vantagens da associação DC – MT, explora-se a alternativa ainda de menor custo e maior disponibilidade, IP – resistividade DC, exemplificando-a com um caso real brasileiro. Esta associação sempre apresentará vantagens sobre a resistividade DC sozinha, pelo simples fato de acrescentar dados de mais um experimento à solução do modelo geoelétrico.
Sem dúvida, a maior vantagem da aplicação do método IP simultaneamente ao de resistividade, continua residindo na possibilidade de existência de camadas IP que não necessariamente constituem camadas de resistividade.

INTRODUCTION

Resistivity, induced polarization (IP) and magnetotelluric (MT) soundings over a horizontally layered Earth model provide information about the distribution of geoelectric properties and thicknesses of the individual layers. These geoelectric properties, primarily resistivity and chargeability, are estimated from the measured apparent surface values prior to interpretation. It is well known (Slichter, 1933; Stevenson, 1934) that with an infinite amount of perfectly precise data, 1-D resistivity data should provide a unique model solution. In practice, the ambiguity which arises from inadequate, inaccurate data, as well as from either equivalence or supression of layers (Orellana, 1963, 1972; Zohdy, 1974, 1975) cannot be reduced without additional model information or independent data.

Intuition suggests that if different data sets (preferably involving common parameters but different phenomena) are used, at least some of the ambiguity inherent in each method is reduced. The combination of resistivity and IP pseudo-sections in the interpretation of 2-D structures has been reported by Pelton et al. (1978). Oldenburg (1979) gave solutions to the 1-D MT problem with resistivity data as a constraint. Vozoff & Jupp (1975) combined apparent resistivity data from DC-resistivity and MT sounding to solve for layer resistivities and thicknesses. The aim of the present work is to extend this last study using IP data and investigate the extent to which IP information improves the parameter resolution in a 1-D layered model. Up to four data sets are used in various combinations; apparent resistivity and chargeability from Schlumberger sounding and apparent resistivity and phase from MT sounding.

Automatic interpretation, usually linearised inversion, is now routinely used to solve resistivity, IP and MT problems. The inversion process uses a least-squares criterion for fitting parameters to the data and provides an estimation of the non-uniqueness and reliability of the parameters of the model obtained. When ambiguity takes place, the desired model usually is taken to be the simplest one satisfying the data.

There are two techniques of searching for the optimum model; the first, a random search or Monte Carlo procedure, was applied to MT and EM induction data by Anderssen (1972), Hermance & Grillot (1974) and Hutton & Jones (1979). The second technique, oriented search, embraces several forms of least-squares approach which are based on a subset of generalized linear inverse theory as described by Wiggins (1972). A simple form of oriented search, called ridge regression (Hoerl & Kennard, 1970a, 1970b; Marquardt, 1970), is a suitable procedure for overconstrained problems involving small but non-zero eigenvalues. This situation arises in resistivity, IP and MT soundings; the example used by Inman et al. (1975) uses Schlmberger sounding data over a layered Earth.

THE FORWARD PROBLEM OVER A HORIZONTALLY STRATIFIED EARTH

We first require a calculation of ρ_{aDC}, M_a, ρ_{aMT} and ϕ_{MT} for a model of L layers with resistivities $\rho_1 \ldots \rho_L$, thicknesses $t_1 \ldots t_{L-1}$ and chargeabilities $M_1 \ldots M_L$. As first used by Ghosh (1971 a, b), ρa for the Schlumberger array is a convolution of the resistivity transform T(x) and the inverse filter I(x) (x is the logarithmic spacing and "*" is the symbol for convolution)

$$\rho_a(x) = T(x) * I(x) \qquad (1)$$

and T(x) is commonly computed through a recurrence relation. In the present study we use Seara's filter (Seara, 1977) with 10 samples per logarithmic decade and 139 filter coefficients (Rigoti, 1985). To find the chargeabilities, we follow the mathematical representation of IP as presented by Siegel (1959) and Dixon & Doherty (1977), in which the apparent chargeability is

$$Ma = \frac{\rho_a' - \rho_a}{\rho_a'} \qquad (2)$$

where ρ_a' is the apparent resistivity including the IP effect. One normally computes the numerator of (2) by the transform difference method

$$\rho_a'' = \rho_a' - \rho_a = (T'(x) - T(x)) * I(X); \qquad (3)$$

so one may write (1) as

$$M_a = \frac{\rho_a''}{\rho_a'' + \rho_a} \qquad (4)$$

Cagniard (1953) applied the concept of apparent resistivity to MT sounding and showed that

$$\rho_a(\omega) = \frac{1}{\omega\mu o} \mid Z_1(\omega) \mid^2 \qquad (5)$$

where the surface impedance is defined (e.g. Ward, 1967) as $Z = \mu_o E_x/B_y$, i.e. the ratio of the relevent horizontal electric field and magnetic induction components. The phase lag of B_y with respect to E_x is

$$\phi(\omega) = \frac{180}{\pi} \tan^{-1} [\mathrm{Im}(Z_1)/\mathrm{Re}(Z_1)] \qquad (6)$$

A review of the theory of EM surface wave impedance measurements can be found in Crossley (1981).

THE INVERSE PROBLEM

As mentioned above, the 1-D geoelectric problem is non-unique for several reasons. A particular layer in the model may be undetectable because its effect is within the noise in the data, or equivalent, resulting in ambiguous interpretation. The detectability of a layer is a function of its resistivity contrast with neighbouring layers and of its thickness and depth of burial. The Dar Zarrouk parameters (longitudinal conductance $S=t/\rho$ and transverse resistance $T=t\rho$) have been shown (Maillet, 1947) to provide a useful indicator of equivalence.

Equivalence can also be extended to IP and MT data where the ambiguity for each method varies according to the particular exploration problem. Important factors in determining the contribution of a particular method are the quality of measurement (i.e. the independence, accuracy and coverage of the data) and the possibility of additional constraints being added to the model. Clearly the simultaneous inversion of different (but related) geophysical data sets provides an objective and practical way of using all the information to solve for the parameters of a model. An appropriate and powerful technique which provides the required information on the data and the parameters is singular value decomposition (SVD).

The Least-Squares Solution Using SVD

The derivative matrix A (dimensioned n data x m = 3L-1 parameters) is found by a forward difference approximation, based on appropriate theory for each method. Matrix A can be factored (e.g. Jackson, 1972) into the product

$$A = U_p \Lambda_p V_p^t \tag{7}$$

Here Λ_p is a diagonal matrix containing the p non-zero singular values $\lambda_1, \lambda_2 \ldots \lambda_p$ of A, ordered in decreasing size, U_p is an orthogonal matrix containing the p semi-orthonormalized data eigenvectors and V_p is an orthogonal matrix containing the p semi-orthonormalized parameter eigenvectors.

Let ΔC be the vector containing the differences between observed and calculated data at any iteration an Δ_p be the parameter update vector. The solution of the linearized problem $\Delta C = A\Delta_p$ has the solution

$$\hat{\Delta}_p = V_p \Lambda_p^{-1} U_p^t \Delta C \tag{8}$$

where the identities $U_p^t U_p = V_p V_p^t = I_m$ are appropriate for the overconstrained system $n > m = p$. When some of the eigenvalues are very small, one can either discard parameters or modify solution (8). A popular patch (e.g. Inman, 1975) is to introduce an arbitrary factor K to give the damped least-squares solution

$$\hat{\Delta}_p = (A^t A + KI)^{-1} A^t \Delta C . \tag{9}$$

If we let $B = U_p^t \Delta C$, the equivalent SVD operation (Johansen, 1977) is to add K to each squared eigenvalue of $A^t A$, so

$$\hat{\Delta}_p = \sum_{j=1}^{m} B_j \lambda_j / (\lambda_j^2 + K) V_j . \tag{10}$$

The usual implementation of the SVD algorithm (e.g. Lawson & Hanson, 1974, pp. 110-120) avoids the often ill-conditioned matrix $A^t A$ when finding the eigenvalues and eigenvectors of A; instead it is more efficient to apply Householder transformations directly to A. The advantage of using SVD over (9) is that is provides a more complete statistical and resolution analysis of the problem (it also provides an estimate of the adequate size of the damping factor K).

Weighting Different Data Sets

Particularly with the data sets considered here, the least-squares algorithm must allow for varying dimensions and uncertainties in the measurements. Assuming that the observational errors are statistically uncorrelated, one can introduce a diagonal nxn weighting matrix D whose elements D_{ii} are the inverse of the standard deviation of each of the observed data. This data weighting is equivalent to left multiplication of ΔC and A by D.

In order to compensate for parameters of different dimensions, one can also consider a diagonal parameter weighting matrix W which is designed to avoid bias towards parameters with high values (Wiggins, 1972). The effect of this weighting is to right multiply A by W^{-1} and left multiply ΔP by W. Noting that choice of W is arbitrary, for the geoelectric problem an alternative technique is to transform the resistivity parameters to the logarithmic (natural or base 10) domain.

To monitor the progress of the iterations, we follow Inman (1975) in using the residual variance

$$\delta^2 = \frac{(D\Delta C)^t D\Delta C}{n - m} \tag{11}$$

in which $\delta^2 \leq 1$ for a satisfactory termination. At this point the parameter covariance matrix (Jackson, 1972) may be written as

$$\mathrm{Cov}\,(\hat{p}) = \delta^2 (V_p \Lambda_p^{-2} V_p^t) \tag{12}$$

from which a correlation matrix may be easily constructed

$$\mathrm{Corr}\,(\hat{P}_{ij}) = \frac{\mathrm{Cov}\,(\hat{p}_{ij})}{[\mathrm{Cov}\,(\hat{p}_{ii})\ \mathrm{Cov}\,(\hat{p}_{jj})]^{1/2}} \tag{13}$$

The elements of this matrix indicate the linear dependence between the parameters (a measure of equivalence in the geoelectric problem).

Finally we examine the "degraded" parameter resolution matrix

$$R = \sum_{j=1}^{m} \lambda_j^2 / (\lambda_j^2 + \delta^2) V_j V_j^t \tag{14}$$

(Wiggins, 1972), in which we replace δ^2 by the damping factor K at convergence. Clearly if $K \rightarrow 0$, $R \rightarrow I$ and the parameters are perfectly resolved, i.e. the rank of the system is exactly equal to the number of parameters.

Before discussing results, we show a block diagram (Fig. 1) of the algorithm. Other options, in addition to those shown, are (a) inversion of any of the four data sets separetely, as well as any combination of them; (b) choice of individual data weighting or a fixed percentage; (c) fixing any of the parameters, and (d) fixing the total depth. Note that Test 3 signifies a specified minimum residual variance or a specified maximum number of iterations.

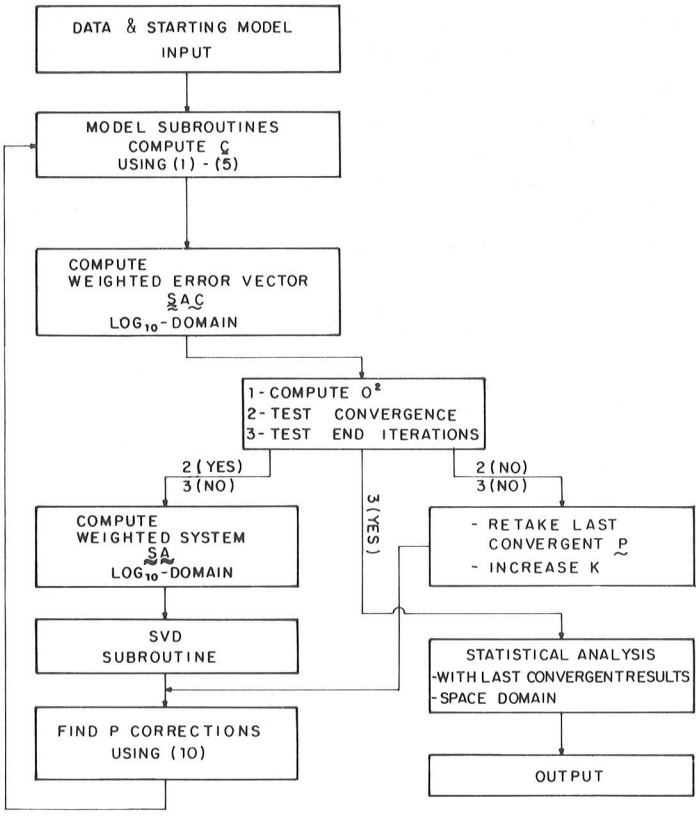

Figure 1 – Block diagram of joint inversion algorithm.

SYNTHETIC MODEL RESULTS

We choose a high-equivalence geoelectric model to study the individual contribution of each method. The purpose is to solve for a thin resistive and polarizable layer for a model in which the 2nd layer is obviously T-equivalent to the first (Table 1). Zohdy's equivalence (Zohdy, 1974) indicates that we can decrease both t_1 and ρ_2 and still fit the data within a prescribed error. We therefore expect that a large uncertainty will appear in the estimated parameters and strong correlations between certain parameters.

Table 1 – Synthetic model parameters – (units apply to all tables)

LAYER	ρ (Ω.m)	t (m)	M (mV/V)	S (= t/ρ)	T (= tρ)
1	10.	100.	10.	10.	1000.
2	100.	10.	25.	0.1	1000.
3	10.		10.		

Using this model, ρ_{aDC}, M_a, ρ_{aMT} and ϕ_{MT} sounding data were calculated at 10 samples per logarithmic decade for either spacing (AB/2) or frequency, as appropriate. Then 1% random values were added to the data, to provide a known problem variance for terminating the iterations. The purpose of this example is to estimate the contribution of each method in finding a thin resistive and polarizable layer. Figs. 2 and 3 show the four data sets, plotted with the best fit theoretical curves as solid lines. It can be seen that the MT data are poorly sensitive to this particular model.

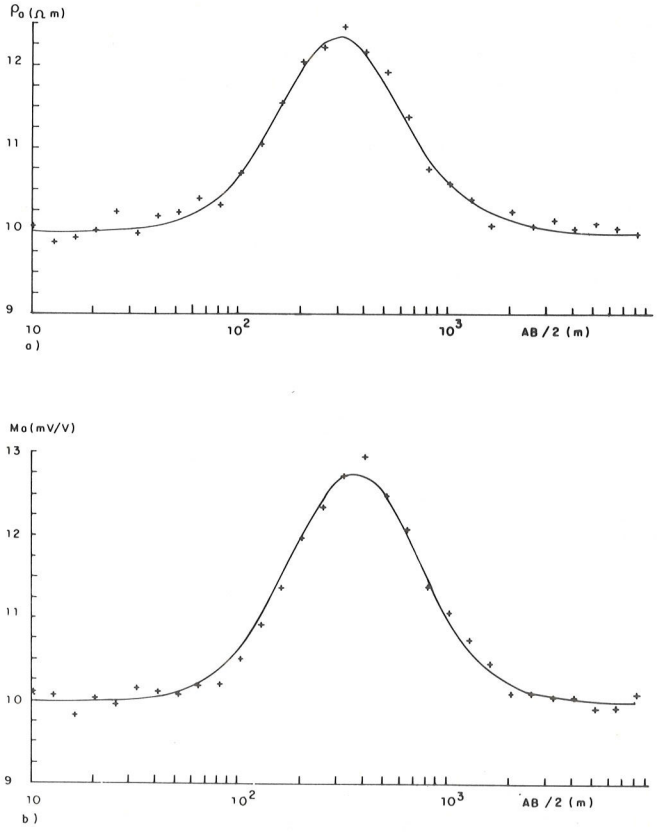

Figure 2 – Observed and calculated Schlumberger data - Case C6 (a) ρ_{aDC} (b) M_a (+ = field data, solid line = best fit).

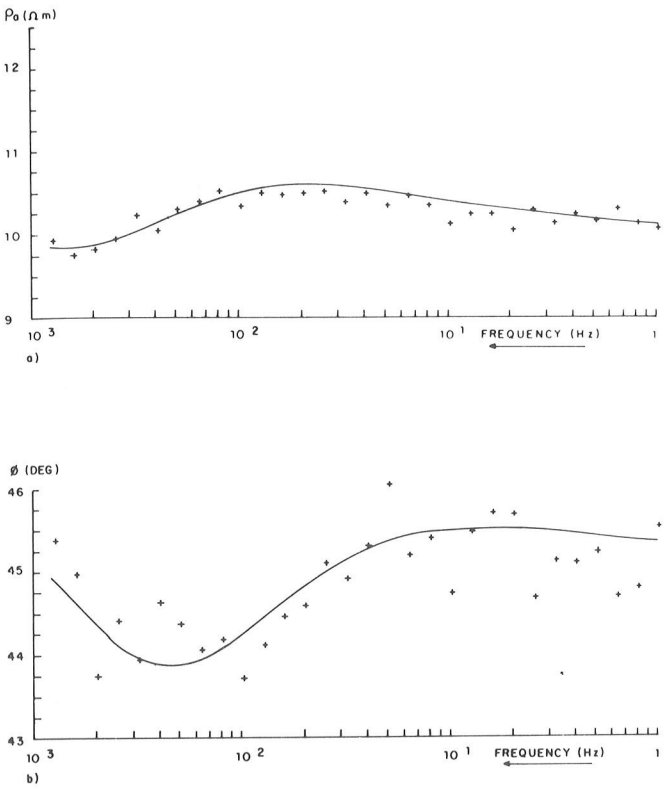

Figure 3 – Observed and calculated MT data - Case C6 (a) ρ_{aMT} (b) Phase ϕ (+ = field data, solid line = best fit).

We remark here that the choice of the starting model (Table 2) was not intended to test the efficiency of the inversion algorithm. Also, we were not concerned with the overall fit of the data but more with the strong equivalence (non-uniqueness) of the second layer. Furthermore, the ist and 3rd layer resistivities and chargeabilities are asymptotically well defined at small and large electrode spacings (or frequencies) and can always be determined independently of the starting model. Ambiguity in the present case then involves only ρ_2, t_1, t_2 and M_2. Starting with the same initial parameters, seven cases of inversion were run (Table 3).

Table 2 – Initial parameters for synthetic model

LAYER	ρ	t	M
1	10.	50.	10.
2	50.	50.	15.
3	10.		10.

Table 3 – Combinations of data sets for synthetic model (⋆ = Includes)

	Schlumberger		MT	
Case	ρ_a	M_a	ρ_a	ϕ
C1	–	–	⋆	–
C2	–	–	⋆	⋆
C3	⋆	–	–	–
C4	⋆	⋆	–	–
C5	⋆	⋆	⋆	–
C6	⋆	⋆	⋆	⋆
C7	⋆	–	⋆	⋆

Contribution of Different Data Sets

A discussion of the eigenvalues of this problem and their significance is given in Rigoti (1985) but to conserve space this will not be reproduced here. Fig. 4 shows the plot of the information density vector, i.e. the normalized diagonal elements of S = AH (Jackson, 1972; Crossley & Ried, 1982) for the case C6 when we have the joint inversion of all 4 data sets. One can see that ρ_{aDC}, M_a and ρ_{aMT} data furnish approximately the same information while the ϕ_{MT} data provide information of an order of magnitude smaller.

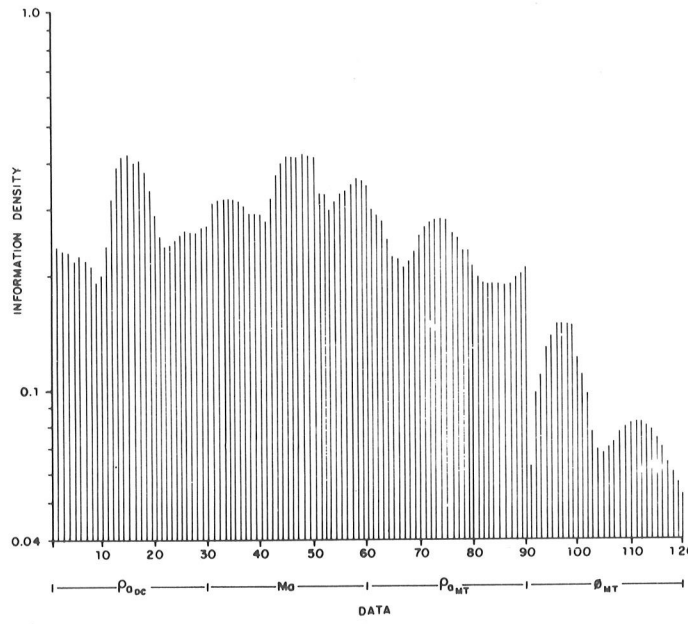

Figure 4 – Information vector for all data sets (case C6, Table 3).

Let us consider parameter resolution, equation (14). Examination of the R matrix (Rigoti, 1985) shows that the parameters ρ_1, ρ_3, M_1, M_2 and M_3 are well resolved (elements R_{ij} close to unity) in all cases. However the resolution of parameters ρ_2, t_2 and t_1 is

dependent on the data (Fig. 5). The following observations concerning Fig. 5 can be made:

a. the DC-resistivity data (case C3) as expected, is superior to MT (cases C1 and C2) in resolving the thin resistive layer of this model,
b. the MT phase data (C6 and C7) do not improve the resolution of the model being studied,
c. the chargeability M_a data contribute significantly (case C4) to resolve the thickness t_1, which is related to the decrease of Zohdy's equivalence to be discussed shortly. Also, observing case C4, there is considerable decrease in ρ_2 resolution, showing that IP is not helping in resolving the classic equivalence,
d. in case C5, when ρ_{aMT} is added to ρ_{aDC}, the resolution of ρ_2 improves significantly thus confirming the utility of MT in this model.

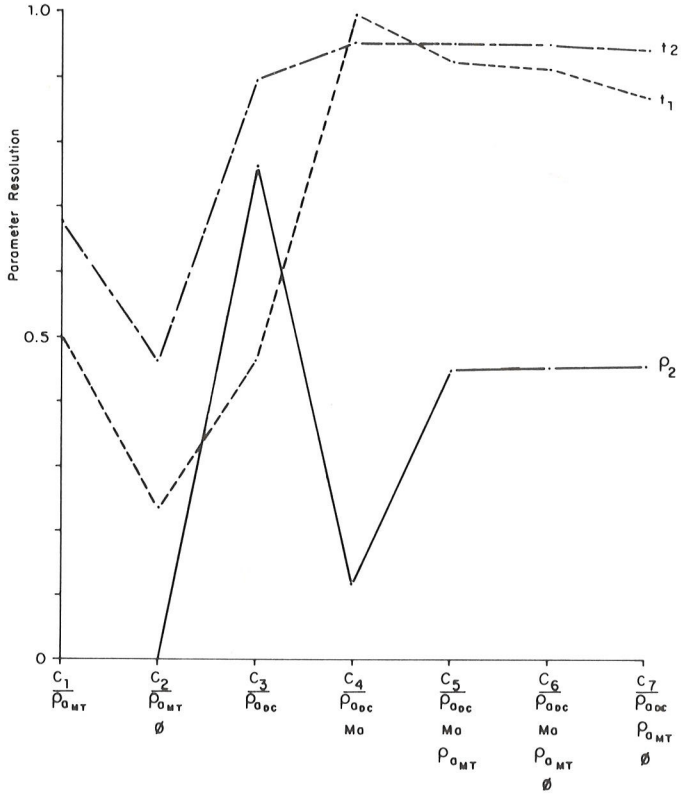

Figure 5 – Parameter resolution (diagonal elements of R, equation (14)) for all combinations of data.

These results show that DC-resistivity combined with MT resistivity is the most effective combination. To emphasize these observations we briefly consider the $\rho_2 - t_2$ and $\rho_2 - t_1$ equivalences.

Zohdy's Equivalence

The correlation between t_1 and ρ_2 shown in Fig. 6a demonstrates the degree of linear dependence between the two parameters. The positive correlation factor indicates that each parameter can be varied proportionally (within a certain range) and the data fit will still be within the limits of error of the data. This correlation factor (close to 1 for C2 and C3) decreases considerably in case C4 and approaches zero in the remaining cases. When the chargeability data are removed in C7 there is little change in the value of correlation.

The standard deviations of parameter t_1 demonstrate approximately the same behavior as the correlation above; the only difference is that in case C4, t_1 is as accurate as in cases C5-C7 (Rigoti, 1985).

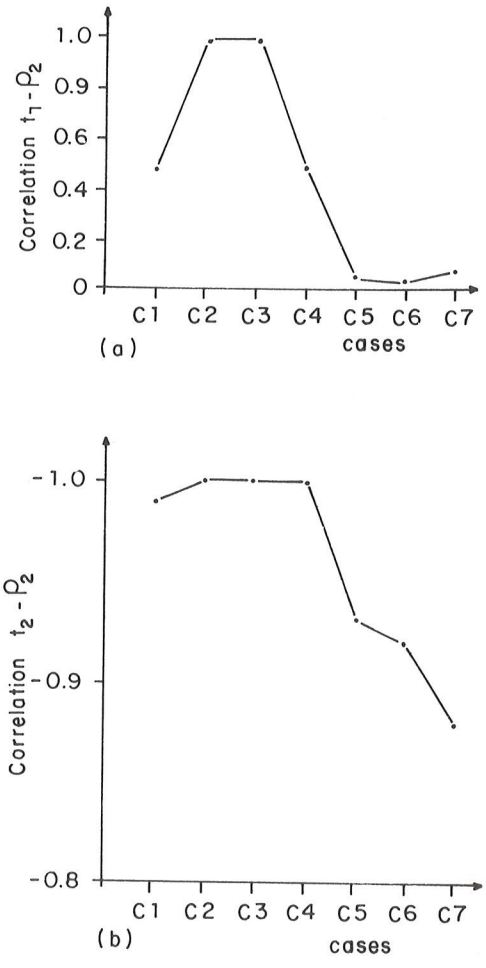

Figure 6 – Illustration of equivalence (a) Zhody's equivalence, correlation t_1 - ρ_2 (b) classic equivalence, correlation t_2 - ρ_2.

Classic Equivalence

The correlation factor between t_2 and ρ_2 (Fig. 6b) in all cases approaches -1, which indicates that we can vary ρ_2, t_2 almost arbitrarily as long as $\rho_2 t_2$ is approximately constant, and still preserve the data fit within the error. The use of all four data sets does little to improve this situation.

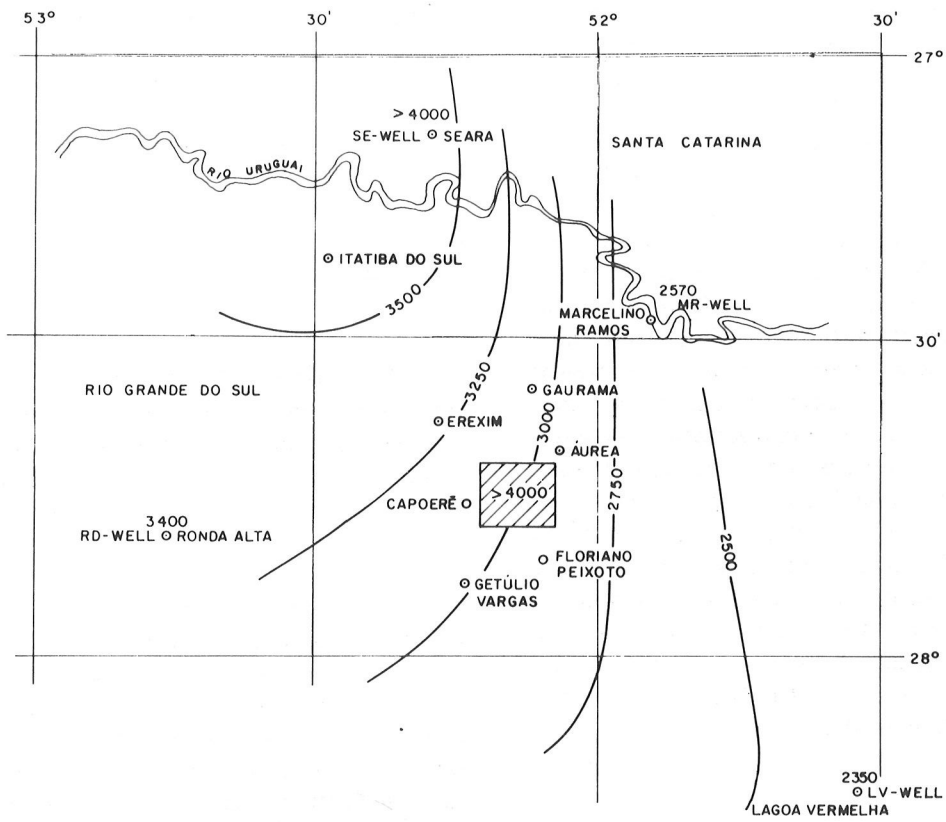

Figure 7 – Site location for field survey showing contours of basement depth from the well log data.

IP-RESISTIVITY FIELD EXAMPLE

We present here an example of a combined DC-resistivity and IP Schlumberger survey, equivalent to case C4 in the previous synthetic model. The survey was carried out to study a morphostructural anomaly in the south of Brazil (Fig. 7) by the Instituto de Pesquisas Tecnológicas do Estado de São Paulo (IPT) for the joint-venture CESP/IPT. The main objective was to determine the depth to the geological basement.

Table 4 – Geolocial units and their geoelectric characteristics as determined from the IP-Resistivity Survey.

Legend	Geological Unit	Depth (m)	Resistivity (Ωm)	Chargeability (mV/V)
V V V V V V V V V V V V V V V V V	Serra Geral Basalts	0 - 850	60 - 600	3 - 30
.–..–..–.. ..–..–..– –..–..–..	Mesozoic-Paleozoic Sedimentary Rocks	850 - 2900	30 - 110	6 - 15
. . . .	Eopaleozoic Sedimentary Rocks (The geological basement)	2900 - 5000?	2 - 10	4 - 8?
+ + + + + + + + + + +	Granitic Electrical Basement	5000? - ∞	> 2000	> 10

The main geological units are given in Table 4. Although the Serra Geral basalts are classified as one geoelectric unit, they are actually a sequence of conductor-resistor beds. The Mesozoic-Paleozoic sedimentary rocks present a continuously decreasing resistivity with depth. Fig. 7 shows the expected depth to the electrical basement derived by interpolation of data from 4 drill holes whose locations are shown.

By contract the survey consisted only of resistivity soundings but as long as the IP readings did not impose operational difficulties they were also taken. The equipment used was a high power transmitter (IPC-7-15 KW – Scintrex) and special care was taken with respect to unpolarizable potential electrodes. The clayey soil assured a very low contact resistance and the resistant basalts kept the signal at adequate levels to provide reliable IP readings up to AB/2 = 3 km. Unfortunately at greater spacing, the measured voltages were inadequate to maintain an acceptable signal/noise ratio, although the resistivity soundings could be taken to a spacing of 10 km. The IP receiver used was the IPR-10 (Scintrex) and the chargeability was taken as M_{32}.

Model Selection

The resistivity sounding curves (Rigoti, 1985) showed that the electrically resistant basement is much deeper than the expected 3 km, which suggests a faulted basement filled in with eopaleozoic sedimentary rocks similar to that occuring in the region of Seara (where the structure was investigated by SE well, Fig. 7). There is no evidence, however, of continuity between the structure being studied and the one occuring in Seara; they are probably restricted molassic basins. From a total of 8 soundings located 4-5 km apart we show here 2 examples: VES-IP/4 and VES-IP/5. The aim of the analysis is to assess the contribution of the IP data in reducing ambiguity in the geoelectric model.

From observed data we generated, according to the procedure given by Orellana (1963), the continuous sounding curves shown in Figs. 8 and 9. Choice of number of layers in the model was estimated using the Dar Zarrouk (DZ) parameters. It is known that these parameters are more reliable estimators of significant layers when the slope of ρ_a is > 0. With this in mind, a DZ point is assigned to each significant inflection point of the curve as shown in Figs. 8 and 9. Each DZ point defines one layer and gives the DZ resistivity ρ_m and DZ depth L_m. Then following Zohdy (1974) one finds the layer resistivities ρ and thicknesses t as shown in Table. 5. Note that we omit the last layer whose effect starts at AB/2 = 8 km (in both soundings) because of the limited data at this separation. One has now a 9-layer starting model for VES-IP/4 and a 6-layer starting model for VES-IP/5 (Table 5), and convergence to a statistically acceptable model is achieved in 5 or 6 iterations in our inversion process.

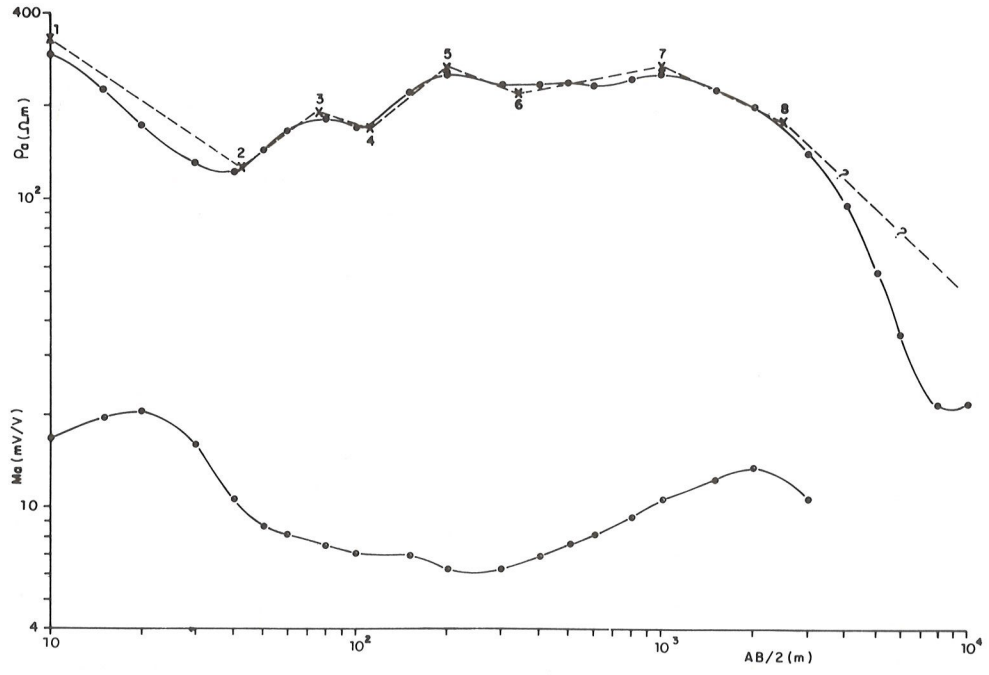

Figure 8 – Field curves for VES-IP/4, dashed line = Dar Zarrouk curve.

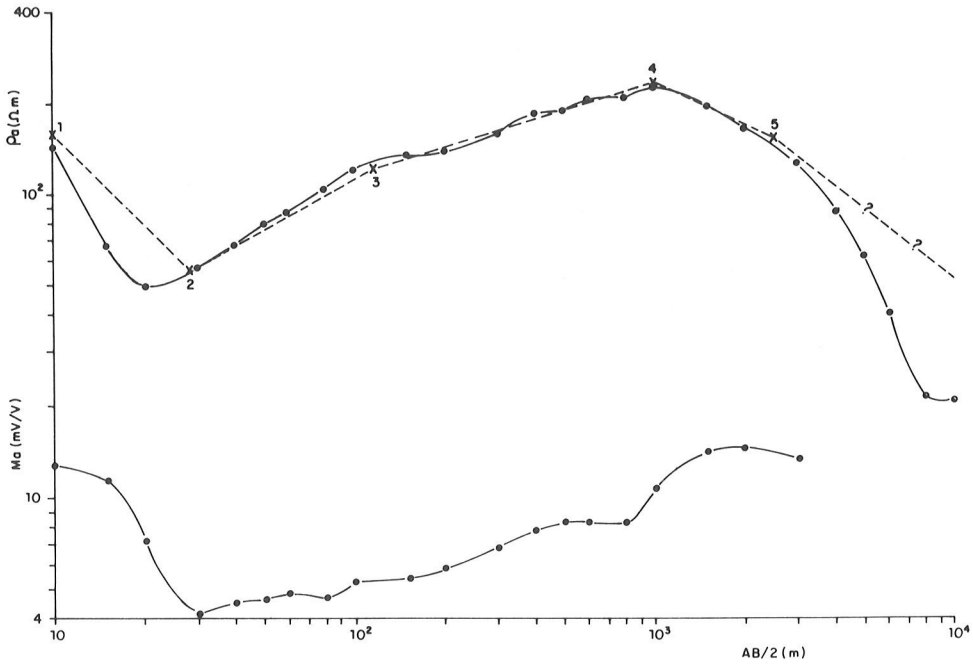

Figure 9 – A Figure 8 for VES-IP/5.

In the case of VES-IP/5 (Fig. 9) it is seen that the chosen DZ curve is reasonably simple, but in the case of VES-IP/4 (Fig. 8) the necessity for layers 3, 4, 5 and 6 can be debated. This sequence presents variations in the DZ curve which do not vary by more than 20% from the mean curve, apart from the possible effects of lateral variations which the 1-D theory cannot account for. The sequence of layers 3, 4, 5 and 6 in VES-IP/4 was replaced by only two layers by taking intermediate points in the DZ function. Both the 9-layer model and the resulting 7-layer model were used as starting models in the inversion. For the IP starting model, inspection of the M_a curves indicated that resistivity layers are also chargeability layers in both soundings, although the M_a curves are probably somewhat simpler.

Table 5 – Estimated model parameters from dar zarrouk curves

Layer	VES - IP/4		VES - IP/5	
	ρ	t	ρ	t
1	330.	10.0	330.	4.0
2	82.3	24.7	23.3	10.6
3	373.	23.9	158.	77.7
4	133.	33.5	253.	856.
5	593.	58.8	108.	1340.
6	163.	130.	< 20.0	
7	301.	649.		
8	133.	1350.		
9	< 20.0			

The observational error may be considerably different for each data set to be considered, so according to the scheme of section 3.2, we must allow for this in the inversion process. The error in the Schlumberger apparent resistivity data, is of order of 3 to 5% and normally it may be considered to be constant for a survey. Between AB/2 = 50 and AB/2 = 200 m in VES-IP/4 (Fig. 8) the ρ_a curve is probably affected by lateral variations so we atributed an error of 7% to the ρ_a data in this interval. For all other ρ_a data the error was assumed to be 3%.

In general, IP measurements are much more dependent on the Instrumentation, electrode contact and background noise because of the low signal (usually ~ 1 mV) being studied in the decay curve. As a consequence, IP sounding data may contain errors varying from 2-3% up to 100%. Assuming a receiver of recent design, over relatively noisy areas, the IP observational error has been found approximately inversely proportional to both measured voltage and chargeability (Rigoti, 1985). The IP data in this survey are more accurate than usual because the natural noise over sedimentary terrains is commonly low, and in the case of this survey, there were high primary voltage and chargeability values with a high signal/noise ratio. With this in mind, an IP data error of approximately 10% was selected for this survey (Rigoti, 1985).

A series of conductor-resistor beds in the basalt renders the geoelectric section highly equivalent and the transition from the resistant basalt to the conductive Mesozoic-Paleozoic sedimentary rocks is another source of high equivalence. There is also a severe problem in discriminating the different Mesozoic-Paleozoic geologic strata because they underlie the thick basalt sequence.

Because the inverse problem admits a large number of solutions, it is necessary to provide some parameter constraints to find the depth of the conductive basement, without necessarily constraining other parameters involved in assessing the relevence of the IP data. For VES-IP/4, both 9 and 7-layer models were used in the inversion with fixed 8th and 6th layer resistivities (100Ωm) respectively. These layers are related to the top part of the Mesozoic-Paleozoic sedimentary sequence. This forces the inversion to find a model with the total thickness of the basalt sequence close to the expected one. Furthermore the total depth to the probable top of the conductive basement (Molassic sediments ?) was fixed at 2800 m within 10%. For VES-IP/5, the 6-layer model had ρ_5 = 90Ωm with the same total depth to the conductive basement (2800 m).

Results for VES-IP/5

Fig. 10 and Table 6 present the final results of the inversions for VES-IP/5 for both resistivity alone and for resistivity combined with IP data (the geological units are in Table 4). It can be seen in Table 6 that although the parameter resolutions are not significantly affected by the inclusion of IP data, the percentage parameter standard deviations are reduced for all parameters except for layer 2 which must be regarded as very tentative. Also the information vectors (Rigoti, 1985) are approximately the same for both resistivity and IP data. Indicating the equal independence of these data sets. Fig. 10 shows that the hypothesis of a conductive basement with the top at about 3 km depth is perfectly valid.

Results for VES-IP/4

This VES clearly warrants a more complex model and we show the results for a 7-layer model in Fig. 11 and Table 7. Inversions of a 10 and a 9-layer model (Rigoti, 1985) provide a similar fit to the data, i.e. the final residual variance is always around 1.0. It has been troublesome to keep the basalt total thickness below 1 km. Also it is impossible to achieve the 3 km depth to the top of the conductive geological basement unless one adds an intermediate resistivity layer of around 30-40Ωm between the fixed ρ_6 = 110Ωm and ρ_7.

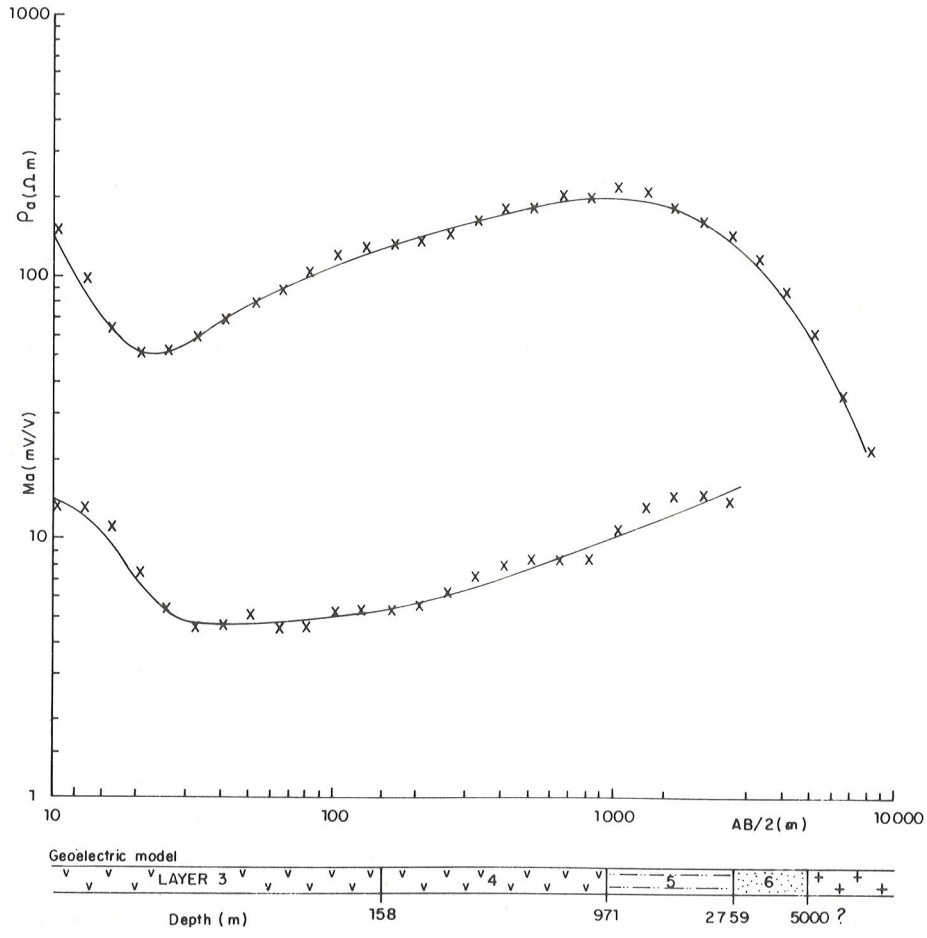

Figure 10 – Joint IP-resistivity Interpretation of VES-IP/5 (x = observed data, solid line = best fit).

Table 6 – VES-IP/5 inversion results: 6-layer model (IP/DC = joint inversion; DC = resistivity alone)

	Parameters		% Standard Deviation		Resolution		
	IP/DC	DC	IP/DC	DC	IP/DC	DC	(%)
ρ_1	358.	406.	9.9	27.	0.97	0.97	
ρ_2	6.1	13.9	880.	510.	0.50	0.51	
ρ_3	164.	165.	9.0	9.3	0.99	0.99	
ρ_4	250.	270.	8.5	16.	0.98	0.96	
ρ_6	6.6	6.1	37.	41.	0.71	0.71	
t_1	4.5	4.2	6.7	26.	1.00	0.99	
t_2	2.3	5.2	890.	530.	0.50	0.49	
t_3	151.	188.	33.	45.	0.78	0.76	
t_4	813.	706.	18.	31.	0.94	0.88	
t_5	1790.	1890.	14.	14.	0.96	0.97	
M_1	15.5		11.		0.99		
M_2	3.9		11.		0.97		
M_3	5.4		11.		0.97		
M_4	11.2		13.		0.96		
M_5	21.2		28.		0.81		
ρ_5	90.0	(fixed)					
M_6	4.0	(fixed)					

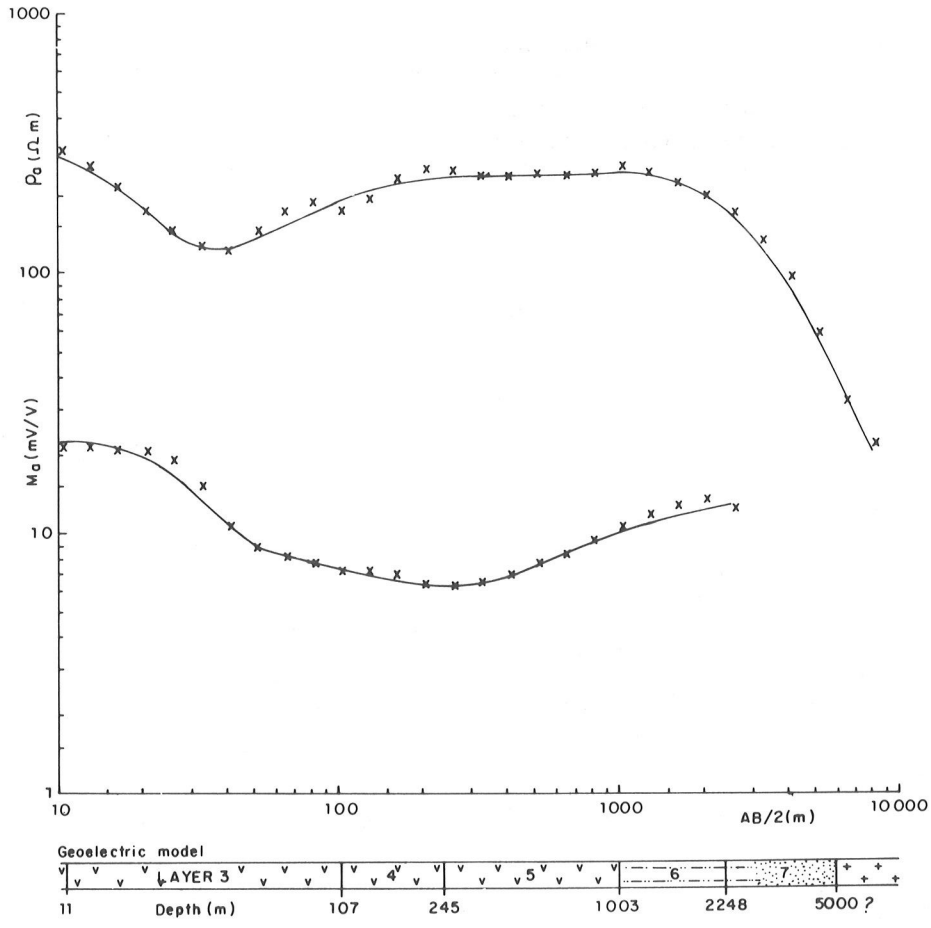

Figure 11 – A Figure 10 for VES-IP/4 with 7-layer model.

Table 7 – VES-IP/4 joint IP-Resistivity inversion: 7 – layer model

Parameters		Standard Deviations (%)	Resolution
ρ_1	323.	14.	1.00
ρ_2	7.0	450.	0.50
ρ_3	333.	260.	0.94
ρ_4	167.	330.	0.81
ρ_5	313.	93.	0.96
ρ_7	11.2	2.0	0.96
t_1	9.8	1.6	1.00
t_2	1.6	100.	0.50
t_3	95.4	210.	0.58
t_4	139.	590.	0.34
t_5	758.	570.	0.87
t_6	1240.	380.	0.92
M_1	23.1	1.8	1.00
M_2	8.9	1.4	0.97
M_3	3.7	4.4	0.86
M_4	6.6	4.9	0.71
M_5	12.7	9.9	0.95
M_6	14.0	63.	0.84
M_7	8.9	600.	0.22E-02
ρ_6	110. (fixed)		

The 7-layer model has approximately the same characteristics as the 6-layer model used in the invesion of VES-IP/5 (which satisfied the hypothesis of a conductive geological basement). One reason for showing VES-IP/4 interpreted with a 7-layer model is because it suggests the possibility of a seventh very conductive layer (ρ approaching zero) able to bring the top of the resistant basement to around 3 km. There is some difficulty in explaining a very low resistivity even with the presence of high salinity water and further there is no indication of a very low resistivity from the available resistivity logs. We did not apply the pseudo-anisotropy corrections because this was replaced by fixing the total depth.

SUMMARY

For current surveys, use of combined MT and DC-resistivity methods is not yet cost effective. Thus we have stressed the importance of the combination of DC-resistivity and IP data which is normally very feasible. In the theoretical 3-layer case presented it was shown that IP data (i.e. apparent chargeability) reduce Zohdy's equivalence thus suggesting that, for a complex model with a large number of layers, the inclusion of IP data would help to interpret DC-resistivity data. This same conclusion was reached after analysing an IP-resistivity field example. In particular the improved confidence in the model parameters would seem to warrant the joint inversion approach where possible.

ACKNOWLEDGEMENTS

We wish to thank IPT for financial support of this project and for permission to publish the results.

REFERENCES

ANDERSEN, R.S., WORTHINGTON, M.H. & CLEARY, J.S. – 1972 – Density modelling by Monte-Carlo inversion. Geophys. J.R. Astr. Soc., **29**:433-444.

CAGNIARD, L. – 1953 – Basic theory of the magnetotelluric method of geophysical prospecting. Geophysics, **18**:605-653.

CROSSLEY, D.J. – 1981 – The theory of EM surface wave impedance mesurements in: Geophysical Applications of Surface Wave Impedance Measurements, L.S. Collet and O.G. Jensen (eds). Geological Survey of Canada, Paper 81-15, 1-17.

CROSSLEY, D.J. & RIED, A.B. – 1982 – Inversion of gamma-ray data for element abundances. Geophysics, **47**:117-126.

DIXON, O. & DOHERTY, J.E. – 1977 – New interpretation methods for IP soundings. Bull. Austr. Soc. Expl. Geophys., **8**:65-69.

GHOSH, D.P. – 1971a – The application of linear filter theory to the direct interpretation of geoelectrical resistivity sounding measurements. Geophys. Prosp., **19**:192-217.

GHOSH, D.P. – 1971b – Inverse filter coefficients for the computation of apparent resistivity standard curves for a horizontally stratified Earth. Geophys. Prosp., **19**:769-775.

HERMANCE, J.F. & GRILLOT, L.R. – 1974 – Constraints of temperatures beneath Iceland from magnetotelluric data, Phys. Earth Planet. Int., **8**:1-12.

HOERL, A.E. & KENNARD, R.W. – 1970a – Ridge regression: biased estimation for nonorthogonal problems. Technometrics, **12**:55-67.

HOERL, A.E. & KENNARD, R.W. – 1970b – Ridge regression: applications to nonorthogonal problems. Technometrics, **12**:69-82.

HUTTON, V.R.S. & JONES, A.G. – 1979 – A multi-station magnetotelluric study in S. Scotland, Geophys. J.R. Astr. Soc., **56**:351-368.

INMAN, J.R. – 1975 – Resistivity inversion with ridge regression. Geophysics, **40**:798-817.

JACKSON, D.D. – 1972 – Interpretation of inaccurate, insufficient and inconsistent data, Geophys. J.R. Astr. Soc., **28**:97-109.

JOHANSEN, H.K. – 1977 – A man/computer interpretation system for resistivity soundings over a horizontally stratified Earth. Geophys. Prosp. **25**:667-691.

LAWSON, C.L. & HANSON, R.J. – 1974 – Solving Least Squares Problems. Prentice-Hall, New Jersey.

MAILLET, R. – 1947 – The fundamental equations of electrical prospecting. Geophysics, **12**:529-556.

MARQUARDT, D.W. – 1970 – Generalized inverses, ridge regression, biased linear estimation and nonlinear estimation. Technometrics, **12**:591-612.

OLDENBERG, D.W. – 1979 – One-dimensional inversion of natural source magnetotelluric observations. Geophysics, **44**:1218-1244.

ORELLANA, E. – 1963 – Properties and drawing of the so called Dar Zarrouk curves. Geophysics, **28**:199-210.

ORELLANA, E. – 1972 – Prospeccion geoelectrica en corriente continua. Paraninfo, Madrid.

PELTON, W.H., RIJO, L. & SWIFT, C.M. – 1978 – Inversion of twodimensional resistivity and induced-polarization data. Geophysics, **43**:788-803.

RIGOTI, A. – 1985 – Reduction of ambiguity in geoelectric models using multiple data sets. M. Sc. thesis, Mc Gill University, Montreal, Canada.

SEARA, J.L. – 1977 – Developments in electrical prospecting methods. M. Sc. thesis, Univesity of Western Ontario, London, Canada.

SIEGEL, H.O. – 1959 – Mathematical formulation and type curves for induced polarization. Geophysics, **24**:547-565.

SLICHTER, L.B. – 1933 – Interpretation of resistivity prospecting for horizontal structures. Physics, **4**:307-332.

STEVENSON, A.F. – 1934 – On the theoretical determination of Earth resistance from surface potential measurements. Physics. **5**:114-124.

VOZOFF, K. & JUPP, D.L.B. – 1975 – Joint inversion of geophysical data, Geophys. J.R. Astr. Soc., **42**:977-991.

WARD, S.H. – 1967 – Electromagnetic Theory for Geophysical Applications. SEG Mining Geophysics, **2**:93-125.

WIGGINS, R.A. – 1972 – The general linear inverse problem; implication of surface waves and free oscillations for Earth structure. Reviews of Geophysics and Space Physics, **10**:251-285.

ZHODY, A.A.R. – 1974 – Use of Dar Zarrouk curves in the interpretation of vertical electrical sounding data. U.S. Geological Survey Bulletin, 1313-D.

ZHODY, A.A.R. – 1975 – Automatic interpretation of Schlumberger sounding curves, using modified Dar Zarrouk functions. U.S. Geological Survey Bulletin, 1313-E.

Versão original recebida em Out./86
Versão final, em Dez./87